

We are IntechOpen, the world's leading publisher of Open Access books Built by scientists, for scientists

6,900

Open access books available

186,000

International authors and editors

200M

Downloads

Our authors are among the

154

Countries delivered to

TOP 1%

most cited scientists

12.2%

Contributors from top 500 universities



WEB OF SCIENCE™

Selection of our books indexed in the Book Citation Index
in Web of Science™ Core Collection (BKCI)

Interested in publishing with us?
Contact book.department@intechopen.com

Numbers displayed above are based on latest data collected.
For more information visit www.intechopen.com



Advances in MR Imaging of Leukodystrophies

Eva-Maria Ratai¹, Paul Caruso¹ and Florian Eichler²

¹Department of Radiology,

²Department of Neurology,

Massachusetts General Hospital,

Harvard Medical School, Boston, MA,

USA

1. Introduction

Leukodystrophies are hereditary disorders of white matter that impair brain that is initially normally formed and developed (1, 2). They can affect brain myelin throughout life. The disorders are commonly progressive in nature and ultimately fatal. First manifestations are often cognitive deterioration and neuropsychological problems. Motor and balance difficulties occur, as do visual abnormalities. Classic leukodystrophies lead to a vegetative state or death within months to years. In general, the earlier the onset of symptoms, the more progressive the disease course.

Most leukodystrophies are monogenetic disorders. The mutant gene often encodes an enzyme or protein that maintains neuronal and/or glial health and is responsible for regulation of brain metabolism. Many enzymes involved play a role in lipid metabolism. The inability to degrade or synthesize substrate leads to an upstream excess or downstream lack of vital lipids. This can cause a wide range of pathology, from inflammatory demyelination to axonal degeneration and microglial activation. Hence, the often cited prominent demyelination is only one manifestation in leukodystrophies, and myelin-forming oligodendrocytes are not the only cells affected in these disorders.

Yet, there are some common characteristics that distinguish the pathology in leukodystrophies from that of other disorders. MRI has played a seminal role in visualization of the lesion pattern. (3). The demyelinating lesions are usually confluent and symmetric. Many of the classic disorders, such as X-linked adrenoleukodystrophy (X-ALD), metachromatic leukodystrophy (MLD) and Krabbe, show relative sparing of subcortical fibers. Yet again, other disorders have early involvement of the U fibers and other unique characteristics, such as cystic rarefaction and degeneration.

Hereditary disorders that do not show demyelination but rather hypomyelination have come to increasing attention (4). Common neurological features in hypomyelinating disorders are developmental delay, nystagmus, cerebellar ataxia and spasticity. One of the better characterized hypomyelinating disorders is Pelizaeus Merzbacher disease (PMD). Beyond this classic disorder, a multitude of other hypomyelinating disorders exist. Only about half of the patients with evidence of hypomyelination on MRI come to a definitive diagnosis. Yet, specific clinical and MRI features can be pathognomonic and lead to diagnosis.

The current review aims to present the diagnostic MRI lesion patterns of leukodystrophies, as well as the utility of advanced MR techniques. While some of these techniques are already established in clinical practice, others are still experimental in nature and require future validation.

2. Conventional brain MRI lesion patterns in LD

Overall, MR imaging has made an enormous contribution to the field of leukodystrophies due to the precise lesion pattern evident on MRI (5). Many leukodystrophies classically show imaging features that, in some cases, are pathognomonic and, in some cases, highly suggestive of the diagnosis. Both demyelinating and hypomyelinating disorders carry distinct features and are listed in **Tables 1 and 2**. While the patterns of maturation of white matter are similar on T1 and T2 weighted images, white matter appears to mature at a later time on T2 weighted images. This is crucial, as it indicates that T1 weighted imaging may be more sensitive to immature myelin than T2 weighted imaging.

In its most severe form, X-ALD is a lethal neurodegenerative disorder with inflammatory demyelination. Defective peroxisomal beta-oxidation causes accumulation of very long-chain fatty acids (VLCFA) in tissues and plasma, particularly in the nervous system and adrenal glands. At least four clinical phenotypes have been delineated: childhood cerebral (CCALD), adult cerebral, adrenomyeloneuropathy (AMN), and female heterozygotes for X-ALD.

In CCALD, the posterior regions of the brain are involved in 80-90% and the frontal regions are involved in 5-10% (6, 7). The lesion evolves in a symmetric confluent fashion starting in the splenium or genu of the corpus callosum and spreading into the periventricular white matter (**Figure 1**). The arcuate fibers are most often spared. In the acute phase, a garland of contrast enhancement is present. In the final stages, white matter atrophy is seen. The systematic progression has given rise to a scoring system of 34 points (8, 9). This pattern is markedly different than that seen in the adult form of the disease, AMN, a non-inflammatory chronic axonopathy.

In Krabbe disease, the parieto-occipital lesions are also present, although a garland of contrast enhancement is never seen (10, 11). MLD shows more diffuse involvement of both frontal and posterior regions of the brain (12). Involvement of the corpus callosum is seen early, although not as striking as that seen in ALD or GLD. A tigroid pattern is often apparent in the centrum semiovale. In contrast to ALD, the outer subarachnoid spaces are not enlarged in MLD, even in the most advanced stages of disease.

Other disorders have characteristic early involvement of the subcortical fibers. Children with Canavan disease present with an enlarged head (“megalencephaly”), but show less behavioral changes than other leukodystrophies of infancy. (13, 14). Their MRI shows diffuse involvement of white matter including the subcortical U fibers (15). There is also involvement of basal ganglia and other gray matter structures. Alexander disease is another leukodystrophy that often manifests with megalencephaly (16). Imaging studies of the brain typically show cerebral white matter abnormalities, preferentially affecting the frontal region, although unusual variants are coming to increasing attention (17, 18).

The MRI of vanishing white matter disease (VWMD) also has a characteristic pattern. It shows progressive loss of white matter over time on proton density and FLAIR images (19-21). The findings on autopsy confirm the white matter rarefaction and cystic

degeneration suggested by the MRI. Regions of relative sparing include the U-fibers, corpus callosum, internal capsule, and the anterior commissure. The cerebellar white matter and brainstem show variable degrees of involvement but do not undergo cystic degeneration.

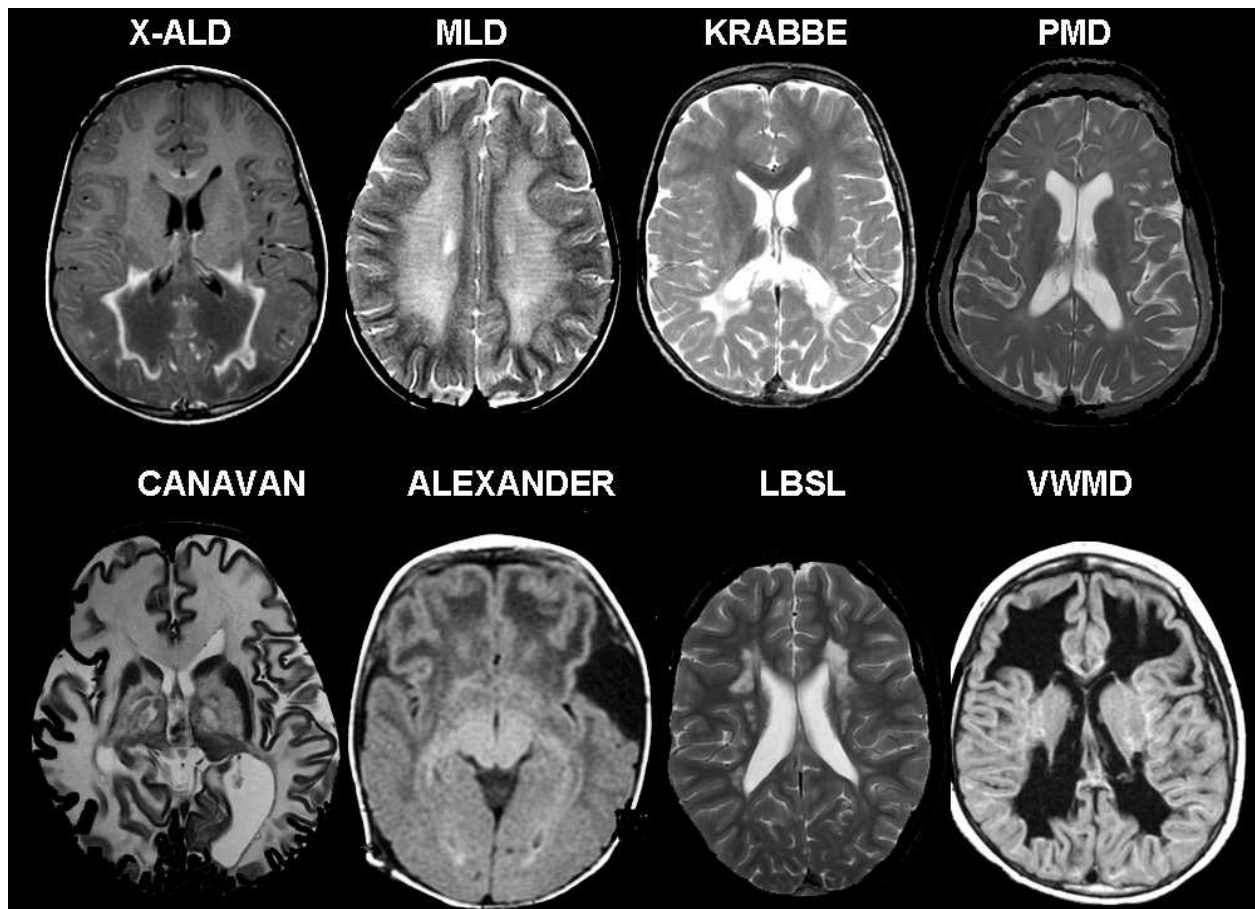


Fig. 1. Lesion Patterns on Conventional MRI in Leukodystrophies and Hypomyelinating Disorders

Brainstem lesion patterns can also often provide critical clues to the diagnosis. Leukoencephalopathy with Brainstem and Spinal Cord Involvement and Elevated White Matter Lactate (LBSL) has recently been described and shows distinct involvement of the pyramidal tracts, medial lemniscus, mesencephalic trigeminal tracts, corticobulbar tracts, and superior cerebellar peduncles. (22). Recognition of the distinct lesion pattern led to the identification of the responsible gene *DARS2*, which encodes mitochondrial aspartyl-tRNA synthetase.

In hypomyelinating disorders, the boundaries between gray and white matter often appear “blurred” (4). The T2 hypointensity of the white matter is milder in hypomyelination than in demyelination and other white matter pathology. Overall, the brain MRI in hypomyelination looks like that of a young child, with less well distinguished gray and white matter. As opposed to “delayed myelination,” the pattern on brain MRI is unchanged, as in myelination is “stuck” on two MRIs 6-12 months apart in a child older than one year of age. While at first glance, hypomyelinating disorders may all have a similar MRI

appearance, there are a group of disorders for which the MRI scan can provide clues to the diagnosis (see **Table 2**). In these individual disorders attention to the deep gray matter structures will often reveal a characteristic “signature” (4).

<i>Leukodystrophy</i>	<i>Mutated genes</i>	<i>Characteristics on Brain MRI</i>
Aicardi-Goutières syndrome (78, 79)	TREX1	Often with microcephaly and intracranial calcifications (CT)
Alexander Disease	GFAP	Macrocephaly with frequent frontal lesion predominance in childhood, variants with abnormalities in medulla and spinal cord, ventricular garlands
Canavan Disease	ASPA	Macrocephaly, subcortical U fibers and basal ganglia involved
Cerebral autosomal dominant arteriopathy with subcortical infarcts and leukoencephalopathy (CADASIL)	NOTCH3	Multiple small hemorrhages. Widened perivascular spaces in the centrum semiovale and basal ganglia
Cerebrotendinous Xanthomatosis	CYP27A1	Cerebellar lesions, calcifications visible on CT
Globoid Leukodystrophy (Krabbe Disease)	GALC	Posterior predominance, no contrast enhancement
Leukoencephalopathy with Brain Stem and Spinal Cord Involvement and Elevated Lactate	DARS2	Characteristic brainstem pattern: pyramidal tracts, cerebellar connections and intraparenchymal trajectories of trigeminal nerve
Megalencephalic Leukodystrophy with Cysts (80, 81)	MLC1, GLIALCAM	Macrocephaly with swelling of cerebral white matter and cystic lesions (bilateral anterior temporal lobes)
Metachromatic leukodystrophy	ARSA	Diffuse with initial subcortical sparing, “tigroid pattern” in centrum semiovale
Vanishing White Matter Disease	EIF2B1-5	Confluent cystic degeneration, white matter signal appears CSF-like
X-Linked Adrenoleukodystrophy	ABCD1	CCALD: posterior predominance with contrast enhancement in acute phase AMN: corticospinal tracts and dorsal columns, no contrast enhancement

Table 1. Characteristics on Brain MRI in Leukodystrophies

<i>Hypomyelinating Disorder</i>	<i>Mutated genes</i>	<i>Characteristics on Brain MRI</i>
Fucosidosis	FUCA1	T2 hypointensity globus pallidus
GM2 gangliosidoses	HEXA, HEXB	T2 hyperintensity in the basal ganglia
Hypomyelination with atrophy of the basal ganglia and cerebellum	unknown	Atrophy of the basal ganglia and cerebellum
Hypomyelination, Hypodontia, Hypogonadotropic Hypogonadism	unknown	Early cerebellar atrophy with absence of putamen
Pelizaeus-Merzbacher Disease	PLP1	Homogeneous T2 hyperintensity of cerebral white matter
Pelizaeus-Merzbacher-like Disease	GJC2, SLC16A2	Pontine T2 hyperintensity

Table 2. Characteristics on Brain MRI in Hypomyelinating Disorders

Advanced magnetic resonance (MR) imaging techniques, such as proton MR spectroscopic and diffusion tensor (DT) MR imaging, permit the investigation of changes in metabolite levels and water diffusion parameters in leukodystrophy patients. Both metabolite measures and water diffusion parameters offer an opportunity to assess the degree of axonal loss and demyelination in the leukodystrophies.

3. Proton MR spectroscopy

Magnetic resonance spectroscopy (MRS) offers the unique ability to measure metabolite levels in vivo in a non-invasive manner (23, 24, 25). These metabolite quantifications can be used to identify disease, measure the severity of an injury, or monitor a patient's response to treatment. **Table 3** shows the most well characterized metabolite abnormalities detected by MRS in leukodystrophies.

The resonances seen in the brain by MRS are typically low weight molecules (see Figure 2). In the normal brain, the most prominent peak arises from N-acetylaspartate (NAA) at 2.0 ppm. The other major peaks include creatine (Cr) and phosphocreatine (phospho-Cr), which are observed at 3.0 and 3.3 ppm, respectively, as well as choline containing compounds. ¹H MR spectra acquired with short echo times are characterized by additional resonances from myo-inositol (MI) at 3.5 ppm, and glutamate and glutamine, which overlap with each other so that they are often referred to as Glx, at ~2.5 ppm. Under normal conditions, the lactate concentration is very low in the adult brain. This resonance (observed as a doublet) occurs at 1.32 ppm.

NAA within the adult brain is found exclusively in neurons, serving as a marker of neuronal density and viability and reported to be decreased in a number of neurological disorders.

<i>Leukodystrophy or Hypomyelinating Disorder</i>	<i>Systemic metabolites</i>	<i>Brain metabolites abnormalities on proton MR spectroscopy</i>
Alexander Disease	Unknown	Infantile form: myoinositol elevations in white and gray matter, decreased N-acetylaspartate
Canavan Disease	Urine N-acetylaspartate	Highly elevated N-acetylaspartate
Cerebrotendineous Xanthomatosis	Plasma cholestanol	Lipid peaks seen in cerebellum
Globoid Leukodystrophy (Krabbe Disease)	Plasma glucocerebrosides, psychosine	Choline and myoinositol elevations, decreased N-acetylaspartate
GM2 gangliosidosis	GM2 gangliosides	Infantile: variable choline, myoinositol and N-acetylaspartate. Late onset: decreased N-acetylaspartate
Hypomyelination with atrophy of the basal ganglia and cerebellum	Unknown	Increased myoinositol and creatine
Leukoencephalopathy with Brain Stem and Spinal Cord Involvement and Elevated Lactate	Unknown	Decreased N-acetylaspartate and increased myo-inositol, choline and lactate
Leukoencephalopathy associated with a disturbance in the metabolism of polyols (83, 84)	Arabinitol and ribitol in urine, plasma and CSF	Elevated levels of arabinitol and ribitol (coupled resonances between 3.5 and 4ppm)
Megalencephalic Leukodystrophy with Cysts	Unknown	Decreased ratio of N-acetylaspartate to Creatine
Pelizaeus-Merzbacher Disease	Unknown	Variable reports on changes in N-acetylaspartate and choline
Vanishing White Matter Disease	Decreased ratio of asialotransferrin to transferrin in CSF	Within cystic white matter complete absence of all metabolites
X-Linked Adrenoleukodystrophy	Plasma very long chain fatty acids	CCALD: Choline elevations within normal appearing white matter, elevations of lactate within the lesion. AMN: decreased N-acetylaspartate in adrenomyeloneuropathy

Table 3. Brain Metabolites Abnormalities on Proton MR Spectroscopy

NAA is the source of acetyl in myelin membrane biosynthesis (26) and is coupled to lipid metabolism and energy generation (27). Creatine serves as a marker for energy-dependent systems in cells and it tends to be low in processes that have low metabolism, such as necrosis and infarction. As Cr and phospho-Cr are in equilibrium, the Cr peak is thought to remain stable in size, despite bioenergetic abnormalities that occur with multiple pathologies. Consequently, the Cr resonance is often used as an internal standard.

The choline (Cho) resonance arises from signals of several soluble components that resonate at 3.2 ppm. This resonance contains contributions primarily from glycerophosphocholine (GPC), phosphocholine (PCho), and Cho. Changes in this resonance are commonly seen with diseases that have alterations in membrane turnover and in inflammatory and gliotic processes (28, 29). The function of MI is not fully understood, although it is believed to be an essential requirement for cell growth, an osmolyte, and a storage form for glucose (30). MI is primarily located in glia, and an increase in MI is commonly thought to be a marker of gliosis (31). Lactate is produced by anaerobic metabolism, and increased lactate has been found during hypoxia (32), mitochondrial diseases (33, 34), seizures (35), and in the first hours after birth (36, 37).

In the developing brain, Cho and MI are the dominant peaks in the MR spectrum. Their levels are high compared to Cr. In contrast, NAA levels are low in newborns and increase with age, while Cho and MI decrease with age. During the first 6 months of life, these metabolic changes are most rapid, leveling off at about 30 months of age (50). These changes are crucial, as both hypomyelination and delayed myelination affect changes of these metabolites.

In X-ALD, proton MRS sometimes shows metabolite abnormalities beyond the margins of disease depicted by conventional MR imaging (38). The white matter lesion in children with X-ALD shows reduced NAA/Cr and increased Cho/Cr, MI/Cr and Glx/Cr (30). Spectroscopic changes in normal appearing white matter (NAWM) that precede disease progression in patients with X-ALD have been described (39). The changes are an increase in choline and a decrease in NAA. They occur in areas where subsequent lesion progression is observed, but not in the remainder of the brain. These areas may represent a zone of impending or beginning demyelination.

Adrenomyeloneuropathy (AMN) is the adult variant of X-ALD. The disease pathology is usually limited to spinal cord and peripheral nerves ("pure AMN") but shows cerebral involvement on histopathology. MRS studies showed reduced global NAA/Cho and NAA/Cr compared to controls. These changes are most prominent in internal capsule and parieto-occipital white matter. Decreased ratios of NAA in the absence of Cho/Cr elevation suggest prominent axonal involvement (40). Furthermore, Dubey et al demonstrated that the Expanded Disability Status Scale (EDSS) score inversely correlated with global NAA/Cr, suggesting a potential role of axonal injury in clinical disability in pure AMN. (40). Brain involvement demonstrable by MRI is rare in female subjects heterozygous for X-ALD, including those who have clinical evidence of spinal cord involvement. Nevertheless, NAA levels are reduced in the corticospinal projection fibers in female subjects with normal results on MRI, suggesting axonal dysfunction (41).

Canavan disease is caused by a deficiency in aspartoacylase (ASPA), an enzyme involved in the process of degrading NAA to aspartate and acetate. Deficiency leads to the accumulation of NAA, which impairs normal myelination and results in spongiform degeneration of the brain (42, 43). The elevations in NAA can be detected by MR spectroscopy in vivo (**Figure 2**), a diagnostic clue that can then be confirmed by urine measurement of NAA. The distinctly higher NAA peak can even be detected in the newborn

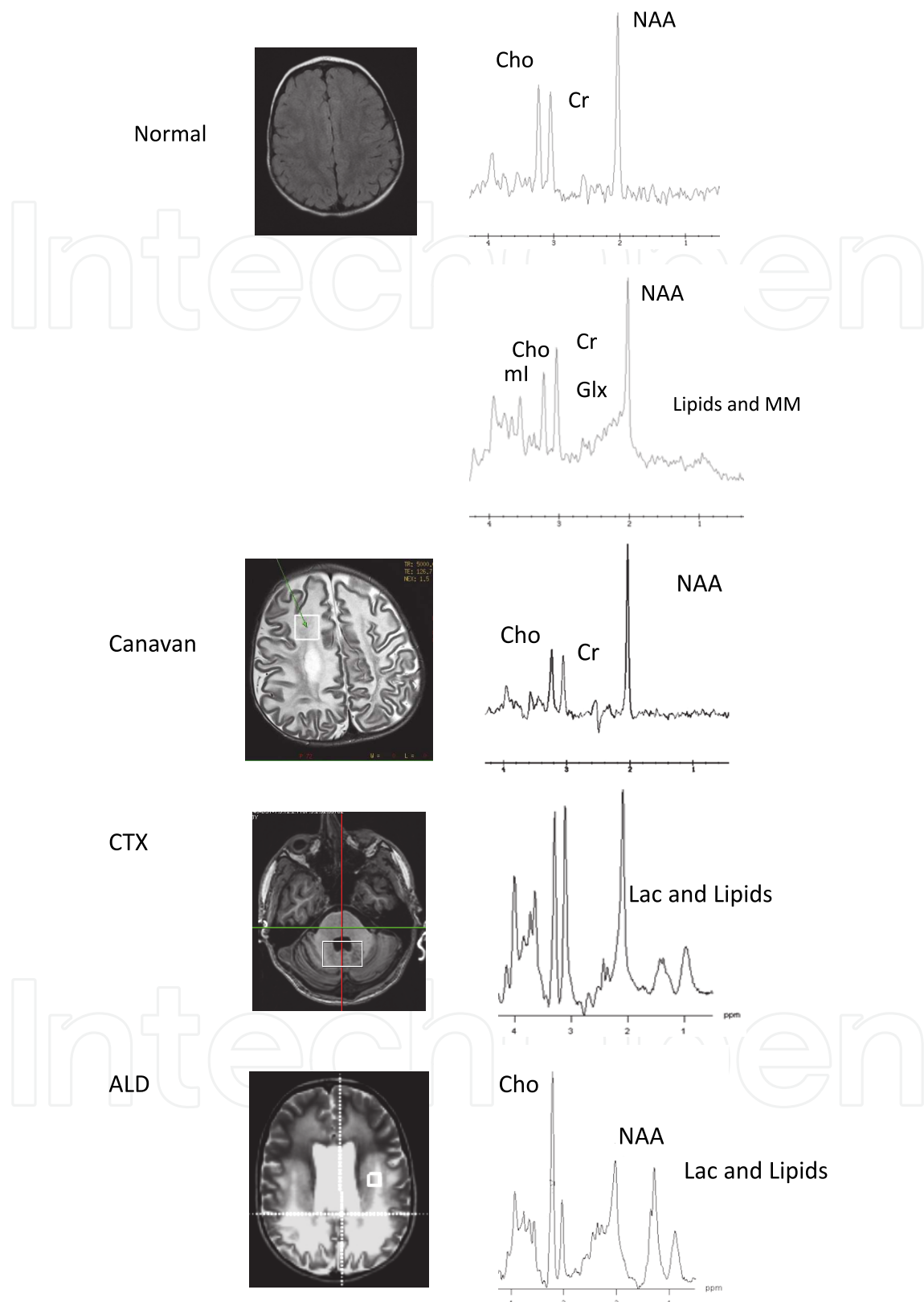


Fig. 2. The spectra of a normal brain are shown at both long echo time (top), TE = 250-280 ms, and short echo time (bottom), TE = 20-50 ms. The spectra for the disease states are as follows: the Canavan spectra are acquired at long echo time, and the ALD and CTX spectra are acquired at short echo time.

although a radiologist only familiar with MR spectra in adults may not recognize the elevation in the newborn as pathologic.

LBSL is a disorder clinically characterized by slowly progressive signs of pyramidal, cerebellar and dorsal column dysfunction. LBSL shows a very distinct MRI pattern, with selective involvement of cerebral and cerebellar white matter and brainstem and spinal tracks, while U-fibers are spared (44). In LBSL, MR spectroscopy characteristically reveals decreased NAA and increased lactate, Cho and MI in the white matter, suggesting axonal damage and gliosis (45). Lately, mutations in the DARS2 gene, which encodes mitochondrial aspartyl-tRNA synthetase, have been identified as the underlying defect.

Cerebrotendinous xanthomatosis (CTX) is a rare but treatable disorder characterized by a defect in the metabolic pathway of cholesterol (46). Symptoms in infancy include diarrhea, cataracts and psychomotor retardation. In adulthood, the spectrum of neurologic dysfunction includes mental retardation leading to dementia, psychiatric symptoms, premature retinal aging, and epileptic seizures. The most distinctive MR imaging abnormalities are bilateral T2 hyperintensities in the dentate nuclei and adjacent cerebellar white matter (47). An MRS study showed a reduction in NAA levels and the presence of a lactate peak (see Figure 2). NAA decreases are attributed to neuroaxonal damage due to neurotoxic deposition of cholesterol (48). A recent case report described the presence of abnormal lipid peaks at 0.9 and 1.3 ppm in the cerebellar hemisphere (49). These peaks can either be attributed to membrane breakdown or they may serve as surrogate markers of major lipid storage, with a potential role in monitoring therapeutic response. In addition, one patient had an increase in MI concentration, pointing to gliosis and astrocytic proliferation (50).

The MR spectra of patients with 4H-Syndrome, a rare form of hypomyelinating leukodystrophy, reveals low Cho/Cr and NAA/Cr, while a prominent MI peak can be observed (51, 52). Low Cho levels are indicative of hypomyelination due to decreased membrane synthesis and turnover. In a new syndrome characterized by Hypomyelination with Atrophy of the Basal Ganglia and Cerebellum (H-ABC), MI and Cr levels are found to be elevated in the cerebral white matter, while NAA and choline levels are normal (53). These findings suggest that neither axonal loss nor active demyelination occurs in the setting of gliosis. In Pelizaeus Merzbacher disease, another hypomyelinating disorder, there have been discrepant reports on metabolite abnormalities detected by MRS. In part, these findings may be explained by the concurrent pathophysiologic processes of hypomyelination, gliosis, and neuronal loss over time (54).

4. Diffusion tensor imaging

While conventional MRI and MR spectroscopy show greatest utility in the diagnoses of leukodystrophies, other techniques, such as diffusion tensor imaging, are starting to be applied to leukodystrophies as well. Diffusion tensor (DT) MRI measures diffusivity of free water molecules in the brain. From the diffusion tensor, one can calculate indices that describe features of the orientationally averaged water diffusivity (isotropic part) and the water molecule displacements affected by the orientation of a regularly ordered structure in the tissue (anisotropic diffusion). Compared to gray matter, in which diffusion shows less directional dependence, white matter apparent diffusion is very anisotropic. (55). This

property, termed fractional anisotropy (FA), depends on the orientation of the white matter tracks and on the degree and integrity of myelination (56-59).

In X-ALD, DT imaging may reflect the different abnormal white matter (AWM) zones in patients with X-ALD (60). We and others have observed that FA decreases and the isotropic apparent diffusion coefficient (iADC) increases over the zones toward the center of the lesion. The decrease in mean FA indicates the loss of an ordered structure governing the directionality of water molecule displacement. The increase in mean iADC suggests an increase in free water and a decrease in structures that restrict water diffusion.

In X-ALD, a strong correlation exists between NAA levels and FA, reinforcing the concept that both reflect axonal integrity. However, proton MR spectroscopic imaging reveals a low NAA level in regions with normal MR and DT imaging findings (61). In contrast, DT imaging showed no abnormalities outside the lesion on T2-weighted images. Further, the membrane turnover and cell accumulation associated with beginning demyelination, recognized in the enhanced choline and creatine signal intensity on proton MR spectroscopic imaging, did not have an effect on diffusion parameters. This suggests that proton MR spectroscopic imaging may have a higher sensitivity than both conventional MR and DT imaging in the early detection of abnormalities related to demyelination or axonal loss in X-ALD patients.

However, in other instances, DTI has proven utility over proton MRSI. In pure AMN patients, DTI-based three-dimensional fiber tracking has shown occult tract-specific cerebral microstructural abnormalities in patients who had a normal conventional brain magnetic resonance image (62). This advance in MR imaging demonstrates that the corticospinal tract abnormalities in AMN reflect a centripetal extension of the spinal cord long-tract distal axonopathy.

DTI anisotropy has also proved useful in Krabbe disease (63, 64). In particular, measurements of white matter metabolites may help assess disease progression and determine optimal candidates for treatment options. Patients with Krabbe disease who underwent stem cell transplantation within the 1st month of life showed substantially smaller decreases in anisotropy ratios than those who were treated later. These findings correlate well with global assessments of disease progression as recognized by neurodevelopmental evaluations and conventional MR imaging.

DT MR imaging studies of cerebral white matter development in human premature and term infants demonstrated that, in general, the apparent diffusion coefficient decreases while relative anisotropy increases with brain maturation. The most prominent regional difference at term is the increased relative anisotropy in the internal capsule, indicative of high directionality of diffusion, which could in part be related to myelination. Axonal diameter increases before and during myelination. This diameter change could also contribute in an important way to the diminished water diffusion perpendicular to the orientation of the fiber and thereby contribute to the increase in relative anisotropy. As anisotropy precedes myelination changes seen on conventional imaging, it is expected that quantitative analysis of diffusion parameters would add to the field of hypomyelinating disorders. Yet, little or no data is currently available in this group of disorders. Clearly, more systematic research is needed in regards to hypomyelination and DTI.

5. Recent applications of advanced MR technology

One major technological advance has been imaging at higher field strength. Magnetic resonance imaging at 4 and 7T allows for better visualization of lesion architecture, white matter tracts, and gray-white matter distinction compared with 1.5T. The field of proton MR spectroscopy has also benefited from higher field strength (65, 66). Better spectral resolution results from improved signal-to-noise ratio and chemical-shift dispersion, and this in turn leads to more reliable detection of metabolites such as myoinositol and glutamine.

Using 7T MRSI, decreases in NAA in the cortex of X-ALD patients were detected, which appears greater in male hemizygotes than in female heterozygotes and most pronounced with the occurrence of white matter lesions in males. (66). Although the cytoarchitecture of the cerebral cortex generally appears normal in X-ALD, scattered neuronal loss can be seen in gray matter during a pathologic examination. Both ratios of myoinositol and choline to creatine were found to be higher in normal appearing white matter of adult ALD patients with brain lesions compared to those without lesions. Yet, the interpretation of 7T MRSI data also poses challenges. Voxels close to the scalp show poor water and lipid suppression. Also, the quantification of spectral data in the presence of substantial radiofrequency excitation field (B₁) variations is difficult. Therefore, focus has shifted on using adiabatic pulses to compensate for radiofrequency inhomogeneity and reduce the chemical shift displacement error (67, 68).

Overcoming some of the shortcomings of DTI, novel methods now exist to map complex fiber architectures of white matter and other brain tissues. Diffusion spectrum imaging (DSI) allows resolution of regions of 3 way fiber crossings (69-71). On DTI this was not possible as fiber crossing led to decreases in FA, making it difficult to distinguish pathological changes from normal fiber crossings. The years ahead will likely bring more studies employing DSI in leukodystrophy patients.

Advances have also been in the development of ex vivo MRI and novel magnetic resonance contrast agents for imaging of autopsy specimen. In metachromatic leukodystrophy, postmortem studies have demonstrated the pathological correlate of the "tigroid stripes" characteristically seen on conventional imaging (72). Through direct correlation of postmortem MR imaging on 1 cm thick blocks with neuropathology staining, the authors were able to show that perivascular clusters of glial cells containing lipid material corresponded to the stripes on MRI.

Using contrast agents ex vivo, the corresponding substrate of imaging can be further elucidated. One such example is luxol fast blue that displays a binding affinity for myelinated constituents of the brain (73). The specificity of luxol fast blue for lipid constituents results in an increase in longitudinal and transverse relaxation rates of tissue dependent on myelination status. The relaxation rates of white matter increase sufficiently to permit T₁-weighted images of ex vivo samples that are similar in contrast behavior to T₁-weighted in vivo imaging. The contrast increases in MR images of LFB-stained ex vivo brain tissues enhancing delineation between upper lamina and the more myelinated lower lamina.

Other advances in MR technology have brought great practical benefits. Sedation and anesthesia represent risks in advanced brain disease of LD patients. Using new techniques, such as propeller MRI, it has become possible to oversample k space and, thereby, compensate for motion and allow follow-up MR imaging without sedation (74, 75). As an

alternative to these retrospective motion-correction techniques, it is also possible to prospectively correct motion in structural imaging and single-voxel spectroscopy using image-based navigators (76-78). In patients with more advanced leukodystrophies, these advances may allow for imaging without sedation and thereby give insight into the more advanced stages of disease.

Overall, not one advanced imaging technology is expected to bring about a breakthrough in the leukodystrophies. Rather, the multimodal approach with coregistration of high resolution imaging with advanced spectroscopic and diffusion imaging will lead to new pathophysiological insights in the years to come. Different diseases, varying phenotypes, and stages within the disease will require varying imaging modalities.

6. Conclusions

MRI has allowed for much progress in the field of leukodystrophies. Prior to arrival of MRI, the specific vulnerability of brain white matter was not well understood. Today, MRI has helped define disorders through the recognition of specific lesion patterns and their evolution over time. This has also led to identification of novel leukodystrophies and the genes underlying these disorders. Even in previously well characterized disorders, MRI patterns have shed light on disease mechanisms.

The understanding of the pathology and molecular basis of leukodystrophies has in turn allowed for new insight into the significance of MRI changes and elucidated the capabilities of MR techniques. Brain MRI today is a valuable tool in monitoring disease progression and the success of therapeutic interventions in leukodystrophies. Advances in new techniques encourage a multimodal approach employing a variety of sequences sensitive to different brain tissue characteristics. Together, these techniques will be able to provide clues to the early stages of disease – insight not gained by pathology in the past.

7. References

- [1] Costello DJ, Eichler AF, Eichler FS. Leukodystrophies: classification, diagnosis, and treatment. *Neurologist* 2009;15(6):319-28.
- [2] Kohlschütter A, Bley A, Brockmann K, Gartner J, Krageloh-Mann I, Rolfs A, et al. Leukodystrophies and other genetic metabolic leukoencephalopathies in children and adults. *Brain Dev*;32(2):82-9.
- [3] van Der Knaap MS. *Magnetic Resonance of Myelination and Myelin Disorders*, 3rd edition. 2005.
- [4] Steenweg ME, Vanderver A, Blaser S, Bizzi A, de Koning TJ, Mancini GM, et al. Magnetic resonance imaging pattern recognition in hypomyelinating disorders. *Brain*;133(10):2971-82.
- [5] Schiffmann R, van der Knaap MS. Invited article: an MRI-based approach to the diagnosis of white matter disorders. *Neurology* 2009;72(8):750-9.
- [6] Moser H SK, Watkins P, Powers J, Moser A. *X-linked adrenoleukodystrophy*. 8th ed. New York: McGraw Hill; 2000.

- [7] Melhem ER, Barker PB, Raymond GV, Moser HW. X-linked adrenoleukodystrophy in children: review of genetic, clinical, and MR imaging characteristics. *AJR Am J Roentgenol* 1999;173(6):1575-81.
- [8] Loes DJ, Hite S, Moser H, Stillman AE, Shapiro E, Lockman L, et al. Adrenoleukodystrophy: a scoring method for brain MR observations. *AJNR Am J Neuroradiol* 1994;15(9):1761-6.
- [9] Loes DJ, Fatemi A, Melhem ER, Gupte N, Bezman L, Moser HW, et al. Analysis of MRI patterns aids prediction of progression in X-linked adrenoleukodystrophy. *Neurology* 2003;61(3):369-74.
- [10] Wenger DA, Suzuki Y, Suzuki K. Galactosylceramide lipidosis: globoid cell leukodystrophy (Krabbe disease). 2001:3669-94.
- [11] Loes DJ, Peters C, Krivit W. Globoid cell leukodystrophy: distinguishing early-onset from late-onset disease using a brain MR imaging scoring method. *AJNR Am J Neuroradiol* 1999;20(2):316-23.
- [12] Eichler F, Grodd W, Grant E, Sessa M, Biffi A, Bley A, et al. Metachromatic leukodystrophy: a scoring system for brain MR imaging observations. *AJNR Am J Neuroradiol* 2009;30(10):1893-7.
- [13] Kumar S, Mattan NS, de Vellis J. Canavan disease: a white matter disorder. *Ment Retard Dev Disabil Res Rev* 2006;12(2):157-65.
- [14] Surendran S, Matalon KM, Tyring SK, Matalon R. Molecular basis of Canavan's disease: from human to mouse. *J Child Neurol* 2003;18(9):604-10.
- [15] Janson CG, McPhee SW, Francis J, Shera D, Assadi M, Freese A, et al. Natural history of Canavan disease revealed by proton magnetic resonance spectroscopy (1H-MRS) and diffusion-weighted MRI. *Neuropediatrics* 2006;37(4):209-21.
- [16] van der Knaap MS, Naidu S, Breiter SN, Blaser S, Stroink H, Springer S, et al. Alexander disease: diagnosis with MR imaging. *AJNR Am J Neuroradiol* 2001;22(3):541-52.
- [17] van der Knaap MS, Salomons GS, Li R, Franzoni E, Gutierrez-Solana LG, Smit LM, et al. Unusual variants of Alexander's disease. *Ann Neurol* 2005;57(3):327-38.
- [18] van der Knaap MS, Ramesh V, Schiffmann R, Blaser S, Kyllerman M, Gholkar A, et al. Alexander disease: ventricular garlands and abnormalities of the medulla and spinal cord. *Neurology* 2006;66(4):494-8.
- [19] van der Knaap MS, Barth PG, Gabreels FJ, Franzoni E, Begeer JH, Stroink H, et al. A new leukoencephalopathy with vanishing white matter. *Neurology* 1997;48(4):845-55.
- [20] van der Knaap MS, Leegwater PA, Konst AA, Visser A, Naidu S, Oudejans CB, et al. Mutations in each of the five subunits of translation initiation factor eIF2B can cause leukoencephalopathy with vanishing white matter. *Ann Neurol* 2002;51(2):264-70.
- [21] Leegwater PA, Vermeulen G, Konst AA, Naidu S, Mulders J, Visser A, et al. Subunits of the translation initiation factor eIF2B are mutant in leukoencephalopathy with vanishing white matter. *Nat Genet* 2001;29(4):383-8.
- [22] Scheper GC, van der Klok T, van Andel RJ, van Berkel CG, Sissler M, Smet J, et al. Mitochondrial aspartyl-tRNA synthetase deficiency causes leukoencephalopathy

- with brain stem and spinal cord involvement and lactate elevation. *Nat Genet* 2007;39(4):534-9.
- [23] Barker PB, Horska A. Neuroimaging in leukodystrophies. *J Child Neurol* 2004;19(8):559-70.
- [24] Barker PB, De Stefano N, Gullapalli R, Lin DDM. *Clinical MR Spectroscopy: Techniques and Applications*. 2010.
- [25] Lin A, Ross BD, Harris K, Wong W. Efficacy of proton magnetic resonance spectroscopy in neurological diagnosis and neurotherapeutic decision making. *NeuroRx*, 2(2), 197-214, review (2005).
- [26] Chakraborty G, Mekala P, Yahya D, Wu G, Ledeen RW. Intraneuronal N-acetylaspartate supplies acetyl groups for myelin lipid synthesis: evidence for myelin-associated aspartoacylase. *J Neurochem* 2001;78(4):736-45.
- [27] Moffett JR, Ross B, Arun P, Madhavarao CN, Namboodiri AM. N-Acetylaspartate in the CNS: from neurodiagnostics to neurobiology. *Prog Neurobiol* 2007;81(2): 89-131.
- [28] Pouwels PJ, Kruse B, Korenke GC, Mao X, Hanefeld FA, Frahm J. Quantitative proton magnetic resonance spectroscopy of childhood adrenoleukodystrophy. *Neuropediatrics* 1998;29(5):254-64.
- [29] Tzika AA, Ball WS, Jr., Vigneron DB, Dunn RS, Nelson SJ, Kirks DR. Childhood adrenoleukodystrophy: assessment with proton MR spectroscopy. *Radiology* 1993;189(2):467-80.
- [30] Ross BD. Biochemical considerations in ¹H spectroscopy. Glutamate and glutamine; myo-inositol and related metabolites. *NMR Biomed* 1991;4(2):59-63.
- [31] Brand A, Richter-Landsberg C, Leibfritz D. Multinuclear NMR studies on the energy metabolism of glial and neuronal cells. *Dev Neurosci* 1993;15(3-5):289-98.
- [32] Kreis R, Arciniegua E, Ernst T, Shonk TK, Flores R, Ross BD. Hypoxic encephalopathy after near-drowning studied by quantitative ¹H-magnetic resonance spectroscopy. *J Clin Invest* 1996;97(5):1142-54.
- [33] Castillo M, Kwok L, Green C. MELAS syndrome: imaging and proton MR spectroscopic findings. *AJNR Am J Neuroradiol* 1995;16(2):233-9.
- [34] Mathews PM, Andermann F, Silver K, Karpati G, Arnold DL. Proton MR spectroscopic characterization of differences in regional brain metabolic abnormalities in mitochondrial encephalomyopathies. *Neurology* 1993;43(12):2484-90.
- [35] Breiter SN, Arroyo S, Mathews VP, Lesser RP, Bryan RN, Barker PB. Proton MR spectroscopy in patients with seizure disorders. *AJNR Am J Neuroradiol* 1994;15(2):373-84.
- [36] Barkovich AJ, Miller SP, Bartha A, Newton N, Hamrick SE, Mukherjee P, et al. MR imaging, MR spectroscopy, and diffusion tensor imaging of sequential studies in neonates with encephalopathy. *AJNR Am J Neuroradiol* 2006;27(3):533-47.
- [37] Barkovich AJ, Westmark KD, Bedi HS, Partridge JC, Ferriero DM, Vigneron DB. Proton spectroscopy and diffusion imaging on the first day of life after perinatal asphyxia: preliminary report. *AJNR Am J Neuroradiol* 2001;22(9):1786-94.

- [38] Holshouser BA, Ashwal S, Luh GY, Shu S, Kahlon S, Auld KL, et al. Proton MR spectroscopy after acute central nervous system injury: outcome prediction in neonates, infants, and children. *Radiology* 1997;202(2):487-96.
- [39] Kruse B, Barker PB, van Zijl PC, Duyn JH, Moonen CT, Moser HW. Multislice proton magnetic resonance spectroscopic imaging in X-linked adrenoleukodystrophy. *Ann Neurol* 1994;36(4):595-608.
- [40] Eichler FS, Barker PB, Cox C, Edwin D, Ulug AM, Moser HW, et al. Proton MR spectroscopic imaging predicts lesion progression on MRI in X-linked adrenoleukodystrophy. *Neurology* 2002;58(6):901-7.
- [41] Dubey P, Fatemi A, Barker PB, Degaonkar M, Troeger M, Zackowski K, et al. Spectroscopic evidence of cerebral axonopathy in patients with "pure" adrenomyeloneuropathy. *Neurology* 2005;64(2):304-10.
- [42] Fatemi A, Barker PB, Ulug AM, Nagae-Poetscher LM, Beauchamp NJ, Moser AB, et al. MRI and proton MRSI in women heterozygous for X-linked adrenoleukodystrophy. *Neurology* 2003;60(8):1301-7.
- [43] Tsai G, Coyle JT. N-acetylaspartate in neuropsychiatric disorders. *Prog Neurobiol* 1995;46(5):531-40.
- [44] Grodd W, Krageloh-Mann I, Klose U, Sauter R. Metabolic and destructive brain disorders in children: findings with localized proton MR spectroscopy. *Radiology* 1991;181(1):173-81.
- [45] van der Knaap MS, Scheper GC. Leukoencephalopathy with Brain Stem and Spinal Cord Involvement and Lactate Elevation. 1993.
- [46] Uluc K, Baskan O, Yildirim KA, Ozsahin S, Koseoglu M, Isak B, et al. Leukoencephalopathy with brain stem and spinal cord involvement and high lactate: a genetically proven case with distinct MRI findings. *J Neurol Sci* 2008;273(1-2):118-22.
- [47] Salen G, Berginer V, Shore V, Horak I, Horak E, Tint GS, et al. Increased concentrations of cholestanol and apolipoprotein B in the cerebrospinal fluid of patients with cerebrotendinous xanthomatosis. Effect of chenodeoxycholic acid. *N Engl J Med* 1987;316(20):1233-8.
- [48] De Stefano N, Dotti MT, Mortilla M, Federico A. Magnetic resonance imaging and spectroscopic changes in brains of patients with cerebrotendinous xanthomatosis. *Brain* 2001;124(Pt 1):121-31.
- [49] Pilo de la Fuente B, Ruiz I, Lopez de Munain A, Jimenez-Escrig A. Cerebrotendinous xanthomatosis: neuropathological findings. *J Neurol* 2008;255(6):839-42.
- [50] Embirucu EK, Otaduy MC, Taneja AK, Leite CC, Kok F, Lucato LT. MR spectroscopy detects lipid peaks in cerebrotendinous xanthomatosis. *AJNR Am J Neuroradiol*;31(7):1347-9.
- [51] Outteryck O, Devos D, Jissendi P, Boespflug-Tanguy O, Hopes L, Renard D, et al. 4H syndrome: a rare cause of leukodystrophy. *J Neurol*;257(10):1759-61.
- [52] Wolf NI, Harting I, Boltshauser E, Wiegand G, Koch MJ, Schmitt-Mechelke T, et al. Leukoencephalopathy with ataxia, hypodontia, and hypomyelination. *Neurology* 2005;64(8):1461-4.

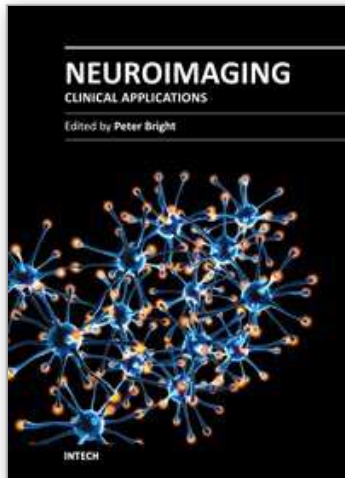
- [53] van der Knaap MS, Linnankivi T, Paetau A, Feigenbaum A, Wakusawa K, Haginoya K, et al. Hypomyelination with atrophy of the basal ganglia and cerebellum: follow-up and pathology. *Neurology* 2007;69(2):166-71.
- [54] Cecil KM. MR spectroscopy of metabolic disorders. *Neuroimaging Clin N Am* 2006;16(1):87-116, viii.
- [55] Basser PJ, Mattiello J, LeBihan D. MR diffusion tensor spectroscopy and imaging. *Biophys J* 1994;66(1):259-67.
- [56] Mori S, Crain BJ, Chacko VP, van Zijl PC. Three-dimensional tracking of axonal projections in the brain by magnetic resonance imaging. *Ann Neurol* 1999;45(2):265-9.
- [57] Wakana S, Jiang H, Nagae-Poetscher LM, van Zijl PC, Mori S. Fiber tract-based atlas of human white matter anatomy. *Radiology* 2004;230(1):77-87.
- [58] Mori S, Oishi K, Faria AV. White matter atlases based on diffusion tensor imaging. *Curr Opin Neurol* 2009;22(4):362-9.
- [59] Wakana S, Caprihan A, Panzenboeck MM, Fallon JH, Perry M, Gollub RL, et al. Reproducibility of quantitative tractography methods applied to cerebral white matter. *Neuroimage* 2007;36(3):630-44.
- [60] Ito R, Melhem ER, Mori S, Eichler FS, Raymond GV, Moser HW. Diffusion tensor brain MR imaging in X-linked cerebral adrenoleukodystrophy. *Neurology* 2001;56(4):544-7.
- [61] Eichler FS, Itoh R, Barker PB, Mori S, Garrett ES, van Zijl PC, et al. Proton MR spectroscopic and diffusion tensor brain MR imaging in X-linked adrenoleukodystrophy: initial experience. *Radiology* 2002;225(1):245-52.
- [62] Dubey P, Fatemi A, Huang H, Nagae-Poetscher L, Wakana S, Barker PB, et al. Diffusion tensor-based imaging reveals occult abnormalities in adrenomyeloneuropathy. *Ann Neurol* 2005;58(5):758-66.
- [63] Escolar ML, Poe MD, Smith JK, Gilmore JH, Kurtzberg J, Lin W, et al. Diffusion tensor imaging detects abnormalities in the corticospinal tracts of neonates with infantile Krabbe disease. *AJNR Am J Neuroradiol* 2009;30(5):1017-21.
- [64] Provenzale JM, Escolar M, Kurtzberg J. Quantitative analysis of diffusion tensor imaging data in serial assessment of Krabbe disease. *Ann N Y Acad Sci* 2005;1064:220-9.
- [65] Oz G, Tkac I, Charnas LR, Choi IY, Bjoraker KJ, Shapiro EG, et al. Assessment of adrenoleukodystrophy lesions by high field MRS in non-sedated pediatric patients. *Neurology* 2005;64(3):434-41.
- [66] Ratai E, Kok T, Wiggins C, Wiggins G, Grant E, Gagoski B, et al. Seven-Tesla proton magnetic resonance spectroscopic imaging in adult X-linked adrenoleukodystrophy. *Arch Neurol* 2008;65(11):1488-94.
- [67] Tannus A, Garwood M. Adiabatic pulses. *NMR Biomed* 1997;10(8):423-34.
- [68] Andronesi OC, Ramadan S, Ratai EM, Jennings D, Mountford CE, Sorensen AG. Spectroscopic imaging with improved gradient modulated constant adiabaticity pulses on high-field clinical scanners. *J Magn Reson*;203(2):283-93.

- [69] Wedeen VJ, Wang RP, Schmahmann JD, Benner T, Tseng WY, Dai G, et al. Diffusion spectrum magnetic resonance imaging (DSI) tractography of crossing fibers. *Neuroimage* 2008;41(4):1267-77.
- [70] Schmahmann JD, Pandya DN, Wang R, Dai G, D'Arceuil HE, de Crespigny AJ, et al. Association fibre pathways of the brain: parallel observations from diffusion spectrum imaging and autoradiography. *Brain* 2007;130(Pt 3):630-53.
- [71] Hagmann P, Sporns O, Madan N, Cammoun L, Pienaar R, Wedeen VJ, et al. White matter maturation reshapes structural connectivity in the late developing human brain. *Proc Natl Acad Sci U S A*;107(44):19067-72.
- [72] van der Voorn JP, Pouwels PJ, Kamphorst W, Powers JM, Lammens M, Barkhof F, et al. Histopathologic correlates of radial stripes on MR images in lysosomal storage disorders. *AJNR Am J Neuroradiol* 2005;26(3):442-6.
- [73] Blackwell ML, Farrar CT, Fischl B, Rosen BR. Target-specific contrast agents for magnetic resonance microscopy. *Neuroimage* 2009;46(2):382-93.
- [74] Tamhane AA, Arfanakis K. Motion correction in periodically-rotated overlapping parallel lines with enhanced reconstruction (PROPELLER) and turbo-prop MRI. *Magn Reson Med* 2009;62(1):174-82.
- [75] Forbes KP, Pipe JG, Karis JP, Farthing V, Heiserman JE. Brain imaging in the unsedated pediatric patient: comparison of periodically rotated overlapping parallel lines with enhanced reconstruction and single-shot fast spin-echo sequences. *AJNR Am J Neuroradiol* 2003;24(5):794-8.
- [76] Hess AT TM, Andronesi OC, Meintjes EM, van der Kouwe AJW. Real-time Motion and B0 corrected single voxel spectroscopy using volumetric navigators. *Magnetic Resonance in Medicine* (in press) 2011.
- [77] Tisdall MD HA, van der Kouwe AJW. Selective k-space Reacquisition in Anatomical Brain Sequences using EPI Navigators. 2010.
- [78] White N, Roddey C, Shankaranarayanan A, Han E, Rettmann D, Santos J, et al. PROMO: Real-time prospective motion correction in MRI using image-based tracking. *Magn Reson Med*;63(1):91-105.
- [79] Orcesi S, La Piana R, Fazzi E. Aicardi-Goutieres syndrome. *Br Med Bull* 2009;89:183-201.
- [80] Uggetti C, La Piana R, Orcesi S, Egitto MG, Crow YJ, Fazzi E. Aicardi-Goutieres syndrome: neuroradiologic findings and follow-up. *AJNR Am J Neuroradiol* 2009;30(10):1971-6.
- [81] Lopez-Hernandez T, Ridder MC, Montolio M, Capdevila-Nortes X, Polder E, Sirisi S, et al. Mutant GlialCAM causes megalencephalic leukoencephalopathy with subcortical cysts, benign familial macrocephaly, and macrocephaly with retardation and autism. *Am J Hum Genet*;88(4):422-32.
- [82] Lopez-Hernandez T, Sirisi S, Capdevila-Nortes X, Montolio M, Fernandez-Duenas V, Scheper GC, et al. Molecular mechanisms of MLC1 and GLIALCAM mutations in megalencephalic leukoencephalopathy with subcortical cysts. *Hum Mol Genet*.

- [83] van der Knaap MS, Wevers RA, Struys EA, Verhoeven NM, Pouwels PJ, Engelke UF, et al. Leukoencephalopathy associated with a disturbance in the metabolism of polyols. *Ann Neurol* 1999;46(6):925-8.
- [84] Moolenaar SH, van der Knaap MS, Engelke UF, Pouwels PJ, Janssen-Zijlstra FS, Verhoeven NM, et al. In vivo and in vitro NMR spectroscopy reveal a putative novel inborn error involving polyol metabolism. *NMR Biomed* 2001;14(3):167-76.

IntechOpen

IntechOpen



Neuroimaging - Clinical Applications

Edited by Prof. Peter Bright

ISBN 978-953-51-0200-7

Hard cover, 576 pages

Publisher InTech

Published online 09, March, 2012

Published in print edition March, 2012

Modern neuroimaging tools allow unprecedented opportunities for understanding brain neuroanatomy and function in health and disease. Each available technique carries with it a particular balance of strengths and limitations, such that converging evidence based on multiple methods provides the most powerful approach for advancing our knowledge in the fields of clinical and cognitive neuroscience. The scope of this book is not to provide a comprehensive overview of methods and their clinical applications but to provide a "snapshot" of current approaches using well established and newly emerging techniques.

How to reference

In order to correctly reference this scholarly work, feel free to copy and paste the following:

Eva-Maria Ratai, Paul Caruso and Florian Eichler (2012). Advances in MR Imaging of Leukodystrophies, Neuroimaging - Clinical Applications, Prof. Peter Bright (Ed.), ISBN: 978-953-51-0200-7, InTech, Available from: <http://www.intechopen.com/books/neuroimaging-clinical-applications/advances-in-mr-imaging-of-leukodystrophies>

INTECH
open science | open minds

InTech Europe

University Campus STeP Ri
Slavka Krautzeka 83/A
51000 Rijeka, Croatia
Phone: +385 (51) 770 447
Fax: +385 (51) 686 166
www.intechopen.com

InTech China

Unit 405, Office Block, Hotel Equatorial Shanghai
No.65, Yan An Road (West), Shanghai, 200040, China
中国上海市延安西路65号上海国际贵都大饭店办公楼405单元
Phone: +86-21-62489820
Fax: +86-21-62489821

© 2012 The Author(s). Licensee IntechOpen. This is an open access article distributed under the terms of the [Creative Commons Attribution 3.0 License](#), which permits unrestricted use, distribution, and reproduction in any medium, provided the original work is properly cited.

IntechOpen

IntechOpen